Nanozyme-Cosmetic Contact Lenses for Ocular Surface Diseases Prevention

Quanyi Liu[a,b], Sheng Zhao[c], Yihong Zhang[c], Qi Fang[a,b], Wanling Liu[c], Rong Wu[a,b], Gen Wei[c], Hui Wei[c,d], and Yan Du[a,b]**

Q.Y. Liu, Q. Fang, R. Wu, Prof. Y. Du

[a]State Key Laboratory of Electroanalytical Chemistry, Changchun Institute of Applied Chemistry, Chinese Academy of Sciences; Changchun, Jilin 130022, China.

[b]School of Applied Chemistry and Engineering, University of Science and Technology of China, Hefei, Anhui 230026, China.

E-mail: duyan@ciac.ac.cn

S. Zhao, Y.H. Zhang, W.L. Liu, G. Wei, Prof. H. Wei

[c]College of Engineering and Applied Sciences, Nanjing National Laboratory of Microstructures, Jiangsu Key Laboratory of Artificial Functional Materials, Nanjing University, Nanjing, Jiangsu 210023, China.

Prof. H. Wei

[d]State Key Laboratory of Analytical Chemistry for Life Science, School of Chemistry and Chemical Engineering, Chemistry and Biomedicine Innovation Center (ChemBIC), Nanjing University, Nanjing, Jiangsu 210023, China.

E-mail: weihui@nju.edu.cn

This article has been accepted for publication and undergone full peer review but has not been through the copyediting, typesetting, pagination and proofreading process, which may lead to differences between this version and the Version of Record. Please cite this article as doi: 10.1002/adma.202305555.

Keywords: nanozymes, reactive oxygen species, Prussian blue analogues, cosmetic contact lens, cornea, ocular surface diseases

Abstract

Efficiently balancing excess reactive oxygen species (ROS) caused by various factors on the ocular surface is a promising strategy for preventing the development of ocular surface diseases (OSDs). Nevertheless, the conventional topical administration of antioxidants is limited in efficacy due to poor absorption, rapid metabolism, and irreversible depletion, which impede their performance. To address this issue, we have developed contact lenses embedded with antioxidant nanozymes that can continuously scavenge ROS, thereby providing an excellent preventive effect against OSDs. Specifically, we chose Prussian blue (PB) family nanozymes based on their multiple antioxidant enzyme-like activities and excellent biocompatibility. The diverse range of colors makes them promising candidates for the development of cosmetic contact lenses (CCLs) as a substitute for conventional pigments. The efficacy of nanozyme-CCLs was demonstrated in rabbits and rats exposed to a high risk of developing OSDs. Our OSDs prevention nanozyme-CCLs can pave the way of CCLs towards powerful wearable biomedical devices and provide novel strategies for the rational utilization of nanomaterials in clinical practice.

1. Introduction

The ocular surface is not only crucial in maintaining normal vision but also serves as a barrier to protect eyes against a diverse range of external insults.[1] However, its delicate architecture and function render it vulnerable to various factors, including air pollution, ultraviolet (UV) radiation, natural aging, and underlying systemic diseases, which can lead to the development of ocular surface diseases (OSDs).[2] Hence, it is imperative to establish preventive and therapeutic approaches for the management of OSDs, particularly in individuals at high risk of developing OSDs.

Excess reactive oxygen species (ROS) resulting from external stimuli, such as pathogens, air pollution, and UV radiation, have been implicated in the pathogenesis of various OSDs, such as keratitis, conjunctivitis, uveitis, and dry eye syndrome.[2b, 3] Additionally, the age-related decrease in antioxidant enzyme activity can lead to uncontrolled oxidative stress, resulting in excess ROS generation.[2e, 4] Consequently, balancing ROS levels on the ocular surface has become a promising strategy for preventing OSDs caused by various factors. However, topical administration of antioxidants, such as vitamin B12 and visomitin eyedrops, has limited efficacy in preventing OSDs due to poor absorption, irreversible consumption, and rapid metabolism.[5] Alternatively, contact lenses (CLs) can be utilized as a feasible platform for continuous and real-time ROS scavenging by consistent interaction with the ocular surface.[6] Embedding catalytic ROS scavengers into CLs may offer a more effective approach for preventing OSDs compared to traditional antioxidants that are rapidly depleted.

Antioxidant nanozymes (the nanomaterials with intrinsic enzyme-like activity) have been widely used in various biomedical applications due to their superior advantages, such as multifunctionality, multienzyme-like activities, and high stability.[7] To achieve prolonged contact with human tissues, antioxidant nanozymes could be incorporated into hydrogels.[8] The nanozyme-loaded hydrogels with ROS scavenging activities have exhibited remarkable efficacy in the treatment of chronic diabetic wounds, ulcerative colitis, and rheumatoid arthritis [9]. Moreover, embedding catalytic ROS scavengers into hydrogels to develop therapeutic CLs is also feasible[10]. Therefore, we reasoned that the incorporation of antioxidant nanozymes within CLs presents an ideal strategy for preventing OSDs, surpassing the limitations of enzymes and conventional antioxidants. Among the various antioxidant nanozymes, Prussian blue (PB) has emerged as a promising candidate due to its multiple antioxidant enzyme-like activities and excellent biocompatibility.[11] Because of the versatility of nanozymes, the diverse range of colors exhibited by PB nanoparticles (PBNPs) and PB analogues (PBA) make them promising candidates for the development of cosmetic contact lenses (CCLs) as a substitute for conventional pigments. Moreover, a wider range of colors can be customized through

their concentration variation or combination. The replacement of traditional pigments with safer nanozymes can not only mitigate the subclinical inflammatory effects associated with CLs but also circumvent the potential safety risks posed by conventional dyes.[12]

Herein, we developed multicolor nanozyme-CCLs with catalytical ROS scavenging activities by embedding PBNPs and PBAs into the host matrix materials (**Scheme 1a**). The multicolor PB family nanozyme-CCLs exhibited excellent biocompatibility and physical properties comparable to commercial CLs. Notably, the nanozyme-CCLs scavenged excess ROS both *in vitro* and *in vivo* by mimicking antioxidant enzymes. In a murine model exposed to high levels of oxidative stress induced by H_2O_2 and UV exposure, all four types of multicolor nanozyme-CCLs demonstrated efficient protection effect on corneal tissues against potential oxidative damage, thus indicating the feasibility of utilizing PB family nanozymes as an alternative to traditional pigments (**Scheme 1b**). Significantly, the nanozyme-CCLs also exhibited preventive potential in rabbits that were at high risk of developing OSDs, highlighting their potential as a promising alternative to traditional CCLs.

2. Results and discussion

2.1. Synthesis, characterization, and catalytical ROS scavenging activities of PBNPs and PBAs

The PBNPs were synthesized through a coprecipitation procedure involving iron (III) and hexacyanoferrate (II) salt, while the PBAs were prepared using a similar method with cobalt (II), nickel (II), and copper (II) precursors and hexacyanoferrate (III) salt.[13] The aqueous solutions of PBNPs and PBAs (denoted as FeFe, CoFe, NiFe, and CuFe, respectively) with different colors and good dispersity are exhibited in the inset of **Figure S1**.

To clarify the relationship between color and wavelength, their transmittance spectra under the visible light range were collected correspondingly (**Figure S1**).[14] We observed that they exhibited blue, reddish-brown, yellow, and pale yellow colors, respectively. Similar to PBNPs, the bright colored PBAs also demonstrate the potential to function as pigments or ink molecules for diverse applications.[15] Their structures and properties were confirmed by Fourier transform infrared spectra (FT-IR), X-ray diffraction (XRD) patterns, scanning electron microscopy (SEM) images, transmission electron microscopy (TEM) images, dynamic light scattering (DLS), and zeta potential analysis (**Figures S2-S8**).

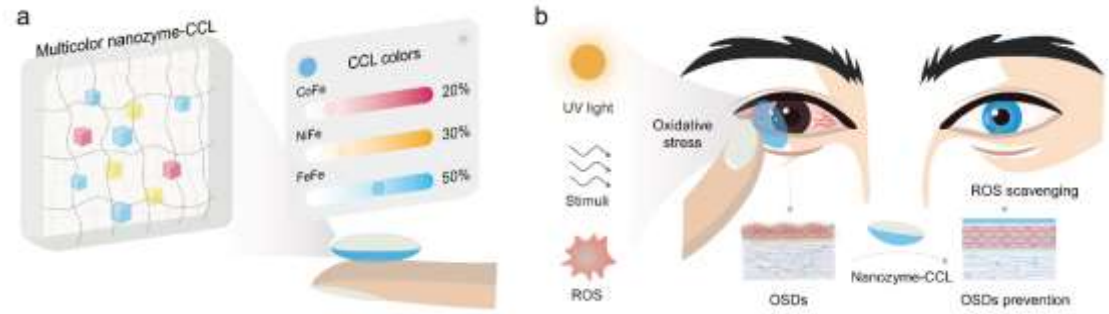

Scheme 1. Schematics of (a) multicolor PB family nanozyme-CCLs and (b) their OSDs prevention applications.

As shown in **Schemes 1b** and **S1**, external stimuli, such as exposure to solar UV radiation, improper CL wearing, and certain pathological conditions, can result in excess ROS generation on the ocular surface to develop OSDs. Generally, superoxide anion radicals ($O_2^{\bullet-}$), hydroxyl free radicals ($^{\bullet}OH$), and hydrogen peroxide (H_2O_2) are three kinds of representative ROS under abnormal physical conditions.[16] Thus, the enzymatic ROS scavenging activities of PBNPs and PBAs toward $O_2^{\bullet-}$, $^{\bullet}OH$, and H_2O_2 were determined to evaluate their potential as antioxidant pigments embedded in CCLs.[11a] As shown in **Figure S9a**, all four kinds of PBNPs and PBAs possessed the ability to scavenge three kinds of typical ROS. Because the structure of PB consists of a three-dimensional network of Fe (III) and $Fe(II)(CN)_6$ units, the cyanide ligands facilitate electron transfer between Fe (II) and Fe (III),

which contributes to PB's exceptional catalytic properties in various applications. The excellent catalase (CAT)- and superoxide dismutase (SOD)-like activities have been attributed to the intervalence charge transfer of an electron from Fe (II) to Fe (III) species within the PB nanozyme.[11a] Because PB and PBAs share the same crystal structure but diverse and metal compositions, we reason that the ROS scavenging activities of PB and PBAs were probably attributed to the abundant redox potentials from the efficient intervalence charge transfer of an electron from different metal (II) to iron (III) species. Because of the differences in redox potentials, which existed between the reduction and oxidation of different PBAs, the enzyme-like activities were not the same. As shown in **Figure S9b**, FeFe possessed better SOD-like activity, while CoFe possessed better CAT-like and $^{\bullet}OH$ scavenging activity (OHS) than other PB family nanozymes (**Figures S9c** and **S9d**). In addition to SOD-like, CAT-like and OHS, glutathione peroxidase (GPx)-like and representative reactive nitrogen species (RNS) scavenging activities were also studied (**Figures S10a**, **S11a** and **S11b**).[17] As shown in **Figures S10b**, **S11c**, and **S11d**, some PB family nanoparticles exhibited significant GPx-like and RNS scavenging activities. The diverse range of colors and catalytic ROS scavenging ability of PB family nanozymes make them promising candidates for the development of multicolor nanozyme-CCLs.

2.2. Preparation and characterization of PB family nanozymes-CCLs

Multicolor nanozyme-CCLs were created by incorporating PB family nanozymes into a biocompatible hydrogel matrix and the matrix was fabricated using clinically approved hydroxyethyl methacrylate (HEMA) (**Figure 1a**).[18] As displayed in **Figure 1b**, the multicolor PB family nanozyme-embedded pHEMA hydrogels could be obtained after free radical polymerization by UV cross-linking. To enhance the hydrophilicity of poly-HEMA (pHEMA)-based CCLs, 1-vinyl-2-pyrrolidinone (NVP) was copolymerized, while ethylene dimethacrylate (EGDMA) and Darocur 2959 were used as the linker and photoinitiator, respectively (**Scheme S2**). During the fabrication process of CCLs, a mixture of HEMA, NVP, EGDMA, Darocur 2959 and different kinds of PB family nanozymes were dropped into a mold of human CLs (**Figure 1a**). Under irradiation with UV light, nanozyme-embedded CCLs (denoted as FeCCL, CoCCL, NiCCL, and CuCCL) with different colors were obtained due to the loading of

multicolor PB family nanozymes (**Figure S12**). Furthermore, to confirm the loading of nanozymes, the obtained CLs (with and without nanozymes) were characterized by FT-IR and X-ray photoelectron spectroscopy (XPS). The existence of PBNPs and PBAs could be proven by the emerging peaks of the C≡N stretching vibration at approximately 2100 cm^{-1} (**Figure 1c**). At the same time, the metal elements could be determined by the overall XPS survey spectra (**Figure S13**) and their corresponding spectra (Fe 2*p*, Co 2*p*, Ni 2*p*, and Cu 2*p*) (**Figure S14**). Fe 2*p* was also confirmed in the PB family nanozyme-CCLs (**Figure S15**), with the C 1*s* spectra of HEMA unchanged (**Figure S16**). The transmittance spectra showed similar characteristics to those of individual PB family nanozymes, proving the origin of the multicolor structure (**Figure S17**). From the comparison of before (**Figure S18**) and after (**Figure 1d**) wearing FeCCL by the same live rabbit, the color of the rabbit right eye was altered from red to blue.

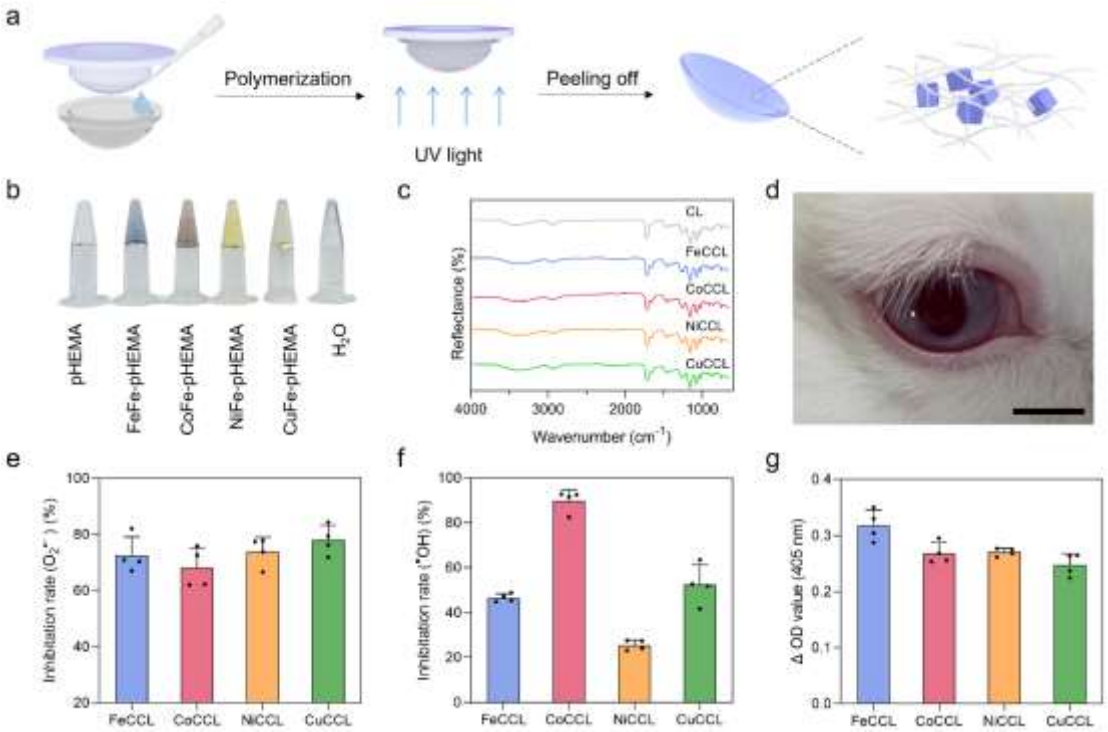

Figure 1. Preparation and characterization of multicolor PB family nanozyme-CCLs. (a) Schematic of the fabrication process of CCLs. (b) Digital photograph of multicolor PB family nanozyme-embedded

pHEMA hydrogels. From left to right: pHEMA, FeFe-pHEMA, CoFe-pHEMA, NiFe-pHEMA, CuFe-pHEMA, and H_2O. (c) FT-IR spectra of PB family nanozyme-CCLs. (d) Digital photograph of the right eye of a live rabbit wearing FeCCL. (Scale bar: 1 cm) (e) $O_2^{\bullet-}$, (f) $^{\bullet}OH$, and (g) H_2O_2 scavenging catalyzed by SOD-like, OHS, and CAT-like activities of nanozyme-CCLs, respectively. The nanozyme-CCLs were prepared using a nanozyme precursor concentration of 0.2 mg mL^{-1}. Data are presented as mean ± SD (n = 4).

With the aid of the mold, the size parameters (diameter: ca. 13.95 mm, base curve: ca. 8.23 mm, central thickness: ca. 0.06 mm, and weight: ca. 14.62 mg) of the obtained CCLs were uniform and suitable for wearing (**Figures S19** and **S20**). There were no significant differences in the water content (ca. 40.61%) and calculated oxygen permeabilities (Dk, ca. 8.41) among different CLs, which all meet the standards for proper wearing (**Figures S21** and **S22**). As depicted in **Figure S23a**, all the nanozyme-CCL samples exhibited swelling behavior similar to that of CLs. This can be attributed to the thin structure of the CCLs, which results in a significant surface area-to-volume ratio, enabling them to achieve complete swelling within 40 s. According to the rheological results (**Figure S23b**), the tan δ values (the ratio of loss modulus and storage modulus) of nanozyme-CCLs remained below one in the frequency range of 0.5 to 10 Hz, indicating their stable behavior as elastic hydrogels. Moreover, the relationship between tan δ values and frequency showed a similar pattern to that of pHEMA with comparable water content, providing further evidence of their remarkable hydrophilicity.[19] Meanwhile, the shade of color could be effectively regulated by the concentration of corresponding PB family nanozymes (**Figure S24**). It is noted that FeFe (blue), CoFe (reddish-brown), and NiFe (yellow) nanozymes could act as three primary colors to provide other hue options (**Figure S25**).[15] As shown in **Figures S26** and **S27**, the dichromatic regulation of the three kinds of PB family nanozymes could afford a series of diverse colors, which could make CCLs more attractive. More colors could be provided by the mixing of two or three PB family nanozymes, which still possessed excellent multienzyme-like activities. Moreover, hue regulation of the multicolor PB family nanozyme-embedded pHEMA could be retained after UV crosslinking (**Figure S28**).

As shown in **Figure S29**, SEM images depicted that most surfaces of the obtained CCLs were smooth, which would not induce mechanical damage to the ocular surfaces and therefore avoid potent corneal abrasions.[20] At the same time, energy dispersive spectroscopy (EDS) further confirmed that nanozymes were embedded uniformly in the CCLs, which ensured that the nanozymes could effectively scavenge excess ROS on the ocular surface (**Figure S30**). Moreover, the hydrophilicity of the nanozyme-CCLs was investigated by water contact angle measurement.[21] As shown in **Figure S31**, the nanozymes could enhance the hydrophilicity (50.1 ± 1.6°, 45.5 ± 1.5°, 54.1 ± 1.9°, 47.4 ± 0.8°, respectively) over the CL control (69.6 ± 2.5°) to endow the CCLs with better wettability.

2.3. ROS scavenging activity of multicolor nanozyme-CCLs

Given the effective ROS scavenging activities of PB family nanozymes, we investigated whether nanozyme-CCLs retained their multienzyme-like activities for regulating oxidative stress. We reasoned that once the lowest concentration exhibits ROS scavenging activities and preventive potential against OSDs, it is expected that higher concentrations will also demonstrate similar or even better effects. Therefore, a nanozyme precursor concentration of 0.2 mg mL^{-1} was chosen for the antioxidant enzyme-like activity test. The SOD-like and OHS activities were studied using the same protocols used for PBNPs and PBAs. In addition, the OHS were also confirmed using electron paramagnetic resonance (EPR) spectroscopy with 5,5-dimethyl-1-pyrroline N-oxide (DMPO) as a trapping agent.[22] A dopamine-enabled assay was performed to evaluate CAT-like activities.[23] As shown in **Figures 1e-g** and **S32**, nanozyme-CCLs still exhibited SOD-like, CAT-like and OHS activities, retaining the capacity to scavenge ROS *in vitro*. The scavenging of ROS occurred at the interface between CCLs and aqueous solution, implying that the nanozyme-CCLs could effectively scavenge excess ROS on the ocular surface via a noninvasive approach.

The stability of nanozyme-CCLs is a prerequisite for further biomedical applications. In this regard, the ROS scavenging activities after long-term storage, xenon lamp exposure, and recycling were investigated.[24] To simulate the real physiological environment of CCLs wearing, an artificial tear fluid (ATF) buffer was used.[25] As shown in **Figures S33a** and **S34a**, the ROS scavenging ability was well maintained after two months of storage in ATF. Moreover, the activities were also preserved after two hours of xenon lamp irradiation, which simulated the solar exposure (**Figures S33b** and **S34b**). Of note, the PB family nanozymes also exhibited acceptable CAT-like activities during three cycles of reuse (**Figure S35**).

2.4. Biocompatibility of multicolor nanozyme-CCLs

After evaluating the ROS scavenging activity of multicolor PB family nanozyme-CCLs, their biocompatibility and biosafety were investigated. The leakage of metal ions from PBNPs and PBAs in CCLs can cause severe damage to the ocular surface; therefore, the release behavior of metal ions was investigated by immersing the CCLs in ATF at 37 °C with shaking at 100 rpm for 2 weeks. We postulate that if the biocompatibility of CCLs is confirmed at high concentrations, it can be extrapolated to other lower concentrations. Accordingly, the CCLs were prepared with a nanozyme HEMA precursor concentration of 1 mg mL^{-1}. The leachates were subsequently analyzed using an inductively coupled plasma atomic emission spectrometer (ICP–AES). Encouragingly, the levels of metal ions in each sample were below the detection limit of the ICP–AES (0.1 ppb) (**Table S1**). These results indicated that PB family nanozymes inside CCLs would remain stable, without any undesirable ion leaching during wearing. The stability of nanozyme-CCLs can avoid potential damage from metal ion leakage, thereby ensuring their biosafety during wearing.

Prior to assessing the cytocompatibility and cytoprotective properties of CCLs, these features of PB family nanozymes were first evaluated. During the wearing process, CCLs come into contact with the corneal epithelium, the outermost layer of the cornea. Therefore, we carefully selected human

corneal epithelial cells (HCECs) as the designated cell line to ensure a faithful representation of the *in vivo* conditions. HCECs were used to construct an intracellular ROS scavenging model by the 2',7'-dichlorodihydrofluorescein diacetate (DCFH-DA) assay to perform the investigation.[26] The Hoechst and DCF fluorescent images and flow cytometry results showed that the intracellular ROS in all the PB family nanozyme groups was significantly lower than that in the H_2O_2 group, suggesting their excellent antioxidant abilities and cytocompatibility at the cellular level (**Figure 2a**, **2b and S36**).[27]

Next, the biocompatibility of nanozyme-CCLs was evaluated by a cell counting kit-8 (CCK-8) assay. Given that CCLs directly interact with HCECs during wearing, their cytocompatibility was also evaluated using HCECs as a model. To mimic the actual working environment of CCLs (only one side would contact the cornea), multicolor PB family nanozyme-embedded pHEMA hydrogels were constructed in 96-well plates, and HCECs were cultured on them (**Figures 2c** and **S37**). Additionally, the coincubation model, where CCLs were directly incubated with HCECs, was also implemented (**Figure 2e**). As depicted in **Figures 2d** and **2f**, none of the four kinds of CCLs exhibited obvious cytotoxicity. The excellent cytocompatibility was derived from the biocompatibility of the pHEMA matrix and PB family nanozymes.[18, 28]

Furthermore, an animal model was established to investigate the *in vivo* biocompatibility of nanozyme-CCLs by embedding various types of CCLs beneath the dorsal skin of C57BL/6 mice.[9b] The CCLs were prepared using a nanozyme precursor concentration of 1 mg mL^{-1}. After 15 days, skin tissues were collected and evaluated for biocompatibility using hematoxylin and eosin (H&E) staining. As shown in **Figure S38**, the histological observations of skin tissue exhibited negligible pathological toxicities and adverse effects in the nanozyme-CCL group. Afterward, commercial CCLs were also evaluated for safety using the same methods to investigate the safety of traditional dyes. As shown in **Figure. S39**, the commercial CCL group exhibited a certain level of inflammation due to dye leakage.

Overall, the above results demonstrated that PB family nanozyme-CCLs were highly biocompatible and could be further utilized for inflammation prevention on the ocular surface *in*

vivo. Furthermore, the comparison with commercial CCLs and previously reported CLs with ROS scavenging ability was listed as **Table S2**.

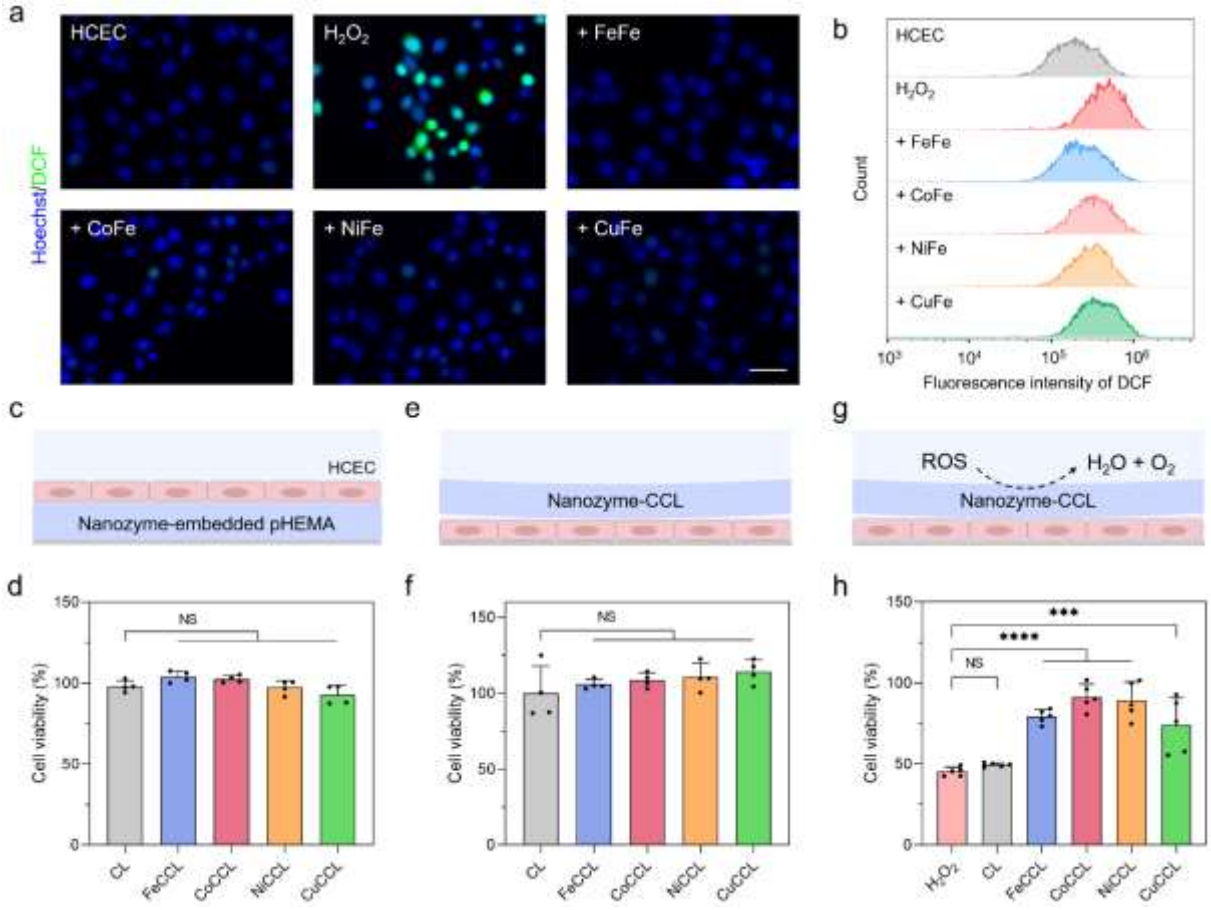

Figure 2. Biocompatibility and cytoprotection of PB family nanozyme-CCLs. (a) Representative DCF (green) and Hoechst (blue) fluorescent staining images of H_2O_2-induced ROS levels in HCECs in the presence of PB family nanozymes and corresponding (b) quantitative analysis of ROS levels by flow cytometry. H_2O_2 group: HCECs without nanozymes treatment. HCEC group: HCECs without H_2O_2 and nanozymes treatment. (Scale bar: 20 μm) (c) Schematic of the incubation of HCECs on nanozyme-embedded pHEMA and the corresponding (d) cell viability. (e) Schematic of the coincubation between HCECs and nanozyme-CCLs and the corresponding (f) cell viability. Data are presented as mean ± SD (n = 4). (g) Schematic of the cytoprotective effect against H_2O_2 and corresponding (h) cell

viability. The nanozyme-CCLs were prepared using a nanozyme precursor concentration of 0.2 mg mL^{-1}. Data are presented as mean ± SD (n = 5). Statistical differences were analyzed by ordinary one-way analysis of variance (ANOVA): ***$P \leq 0.001$, ****$P \leq 0.0001$, and NS (not significant).

2.5. Multicolor nanozyme-CCLs protected cells from ROS *in vitro*

After examining the *in vitro* ROS scavenging activity and biocompatibility of nanozyme-CCLs, we investigated their cytoprotective effect against ROS-induced damage by subjecting HCECs to H_2O_2 treatment.[22] Since the nanozyme-CCLs were applied to the ocular surface, they served as the initial barrier for external ROS stimulation before reaching the cornea. To simulate external stimulation of the cornea, H_2O_2 was first mixed with nanozyme-CCLs and incubated at 37 °C for 24 h. The remaining H_2O_2 was applied to treat HCECs to study the cell viability toward ROS scavenging by nanozyme-CCLs. As shown in **Figures 2g** and **2h**, using the 3-(4,5-dimethyl-2-thiazolyl)2,5-diphenyltetrazolium bromide (MTT) assay, it was found that the nanozyme-CCL group had better cell viability than the H_2O_2 and control (CL) groups, thus demonstrating the excellent cytoprotective ability of multicolor nanozyme-CCLs against external stimulation.

Ultraviolet-A (UVA, 320-400 nm) is approximately 20 times more abundant than UVB (290-320 nm) and comprises over 95% of incident UV radiation.[29] The damage caused by UVA radiation is mediated by its interactions with cellular photosensitizers, which generate ROS and induce subsequent oxidative stress.[30] Thus, departing from the H_2O_2-induced cellular model, the UV-induced cellular model was also constructed to investigate the cytoprotective ability against UV light.[31] As illustrated in **Figure S40a**, HCECs were covered by nanozyme-CCLs to block UV radiation and scavenge the ROS induced by UV light.[11a] The CCK-8 assay results revealed better cell viability in the nanozyme-CCL groups than in the UV and control (CL) groups (**Figure S40b**). We reasoned that the lower cell viabilities in the CoCCL, NiCCL, and CuCCL groups compared to that of the FeCCL group would be caused by the unshielded UV light owing to the mismatch between nanozyme-CCLs and

cell culture wells. Thus, the co-staining with 6-YF488-phalloidin (green) and DAPI (blue) was carried out to investigate the structural integrity of HCECs radiated by UV light (**Figure 3a**).[32] Obvious disruption of the integrity of the cell membranes and changes in cell morphologies could be observed in the UV group compared to those in the HCEC group, suggesting the successful construction of a UV-induced cellular model. The HCECs in the CL group exhibited damage similar to that in the UV group, showing that the pHEMA matrix did not possess cytoprotective ability. In contrast, intact cell structures were observed in different nanozyme-CCL groups, benefiting from the cytoprotective ability of the PB family nanozymes inside.

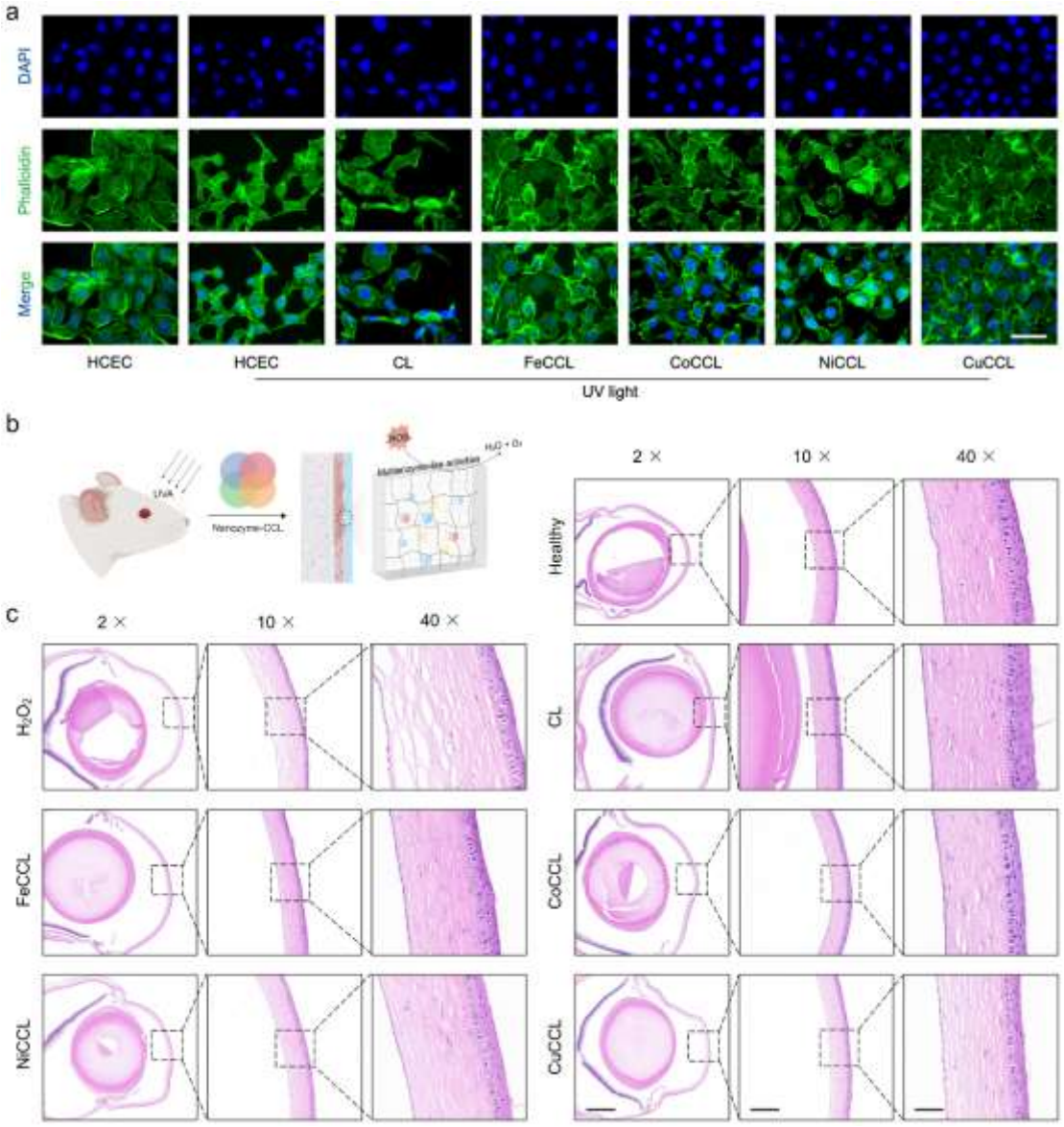

Figure 3. Multicolor PB family nanozyme-CCLs protect the cornea from UV irradiation. (a) Phalloidin (green) and DAPI (blue) fluorescent staining images of HCECs protected by nanozyme-CCLs and the control group (scale bar: 50 μm). (b) Schematic of UV-induced SD rat model for protecting effect evaluation by multicolor PB family nanozyme-CCLs. (c) Representative H&E staining images of corneal tissue of indicated groups (scale bars: 1 mm for 2 ×, 200 μm for 10 ×, and 50 μm for 40 ×). The nanozyme-CCLs were prepared using a nanozyme precursor concentration of 0.2 mg mL^{-1}.

2.6. Multicolor nanozyme-CCLs protected corneas from UV light *in vivo* to prevent OSDs

To prevent OSDs caused by UVA radiation *in vivo*, we reasoned that nanozyme-CCLs could be used due to their ability to scavenge ROS and block UV light. Therefore, we evaluated the performance of nanozyme-CCLs by using a UVA radiation rat model. For the Sprague–Dawley (SD) rat model, smaller CCLs that were suitable for rats were prepared. Before nanozyme-CCLs were worn, a commercial CL care solution was used to treat CCLs to enhance their adhesion and comfort. Simultaneously, sodium hyaluronate eyedrops were dropped into the rat eyes for the same purpose. A UV LED light source with an emission peak of 365 nm was used to mimic external stimulation to construct the OSD model (**Figure 3b**). Then, blue FeCCL, reddish-brown CoCCL, yellow NiCCL, pale yellow CuCCL, or colorless CL was carefully placed on the surface of the eyeballs of SD rats separately.

Following placing multicolor nanozyme-CCLs, the single eye of the rat was irradiated for 45 min, while the rat without placing CLs under UV radiation and healthy rat served as control groups. As the H&E staining images shown in **Figure 3c**, the fibrillar collagen in the corneal stroma was much looser than that of the other groups because of the irritation of UV light, showing the successful establishment of this model. There was no apparent loosening of the arrangement of the corneal stroma in the CL group, indicating that the pHEMA matrix was helpful in shielding against UV irradiation. However, as shown in **Figure S41**, the corneal stromal thickness in the CL group increased compared to that in the healthy and nanozyme-CCL groups. This highlights the importance of nanozymes in protecting the cornea by scavenging ROS.

2.7. Multicolor nanozyme-CCLs protected corneas from ROS-induced damage *in vivo* to prevent OSDs

Based on their excellent bioprotective effect against ROS caused by UV light, the *in vivo* efficacy of nanozyme-CCLs against the high oxidative stress environment was also investigated. To evaluate the OSDs prevention effect of the nanozyme-CCLs *in vivo*, SD rat and rabbit models under the stimulation of H_2O_2 eyedrops were used.[33] Following the same protocols in the UV-induced model, the CCLs were treated with CL care solution. H_2O_2 was applied to the central areas of the eyes to mimic external stimulation before the wearing of multicolor nanozyme-CCLs (**Figure S42**). We reasoned that the multienzyme-like activities of nanozyme-CCLs would endow them with excellent anti-inflammatory abilities to protect corneal tissues.[26] After two days, the eyeballs were collected from the SD rats and stained for H&E evaluation.[32] As the H_2O_2 group shown in **Figure 4a**, the decreased corneal epithelial layer thickness and cell density in the epithelial layer, as well as edema corneal stroma, suggested the successful establishment of a H_2O_2-induced OSD model.[34] The thickness of the corneal epithelial layers in all nanozyme-CCL groups was significantly increased compared to that in the H_2O_2 group, accompanied by increased cell density (**Figures 4b** and **S43b**). Meanwhile, the decreased stromal thickness also proved that multicolor PB family nanozyme-CCLs could protect corneal tissue from excess ROS (**Figure S43a**). As shown in **Figures 4a**, **4b** and **S43**, CL did not exhibit obvious *in vivo* prevention efficacy compared to nanozyme-CCLs. As a result, the prevention efficacy can be attributed to the multienzyme-like PB family nanozyme inside CCLs. To further clarify the mechanism, enzyme-linked immunosorbent assays (ELISAs) were performed to determine three kinds of potential related cytokines, tumor necrosis factor-alpha (TNF-α), interleukin-1beta (IL-1β), and interleukin-10 (IL-10), in extracted corneas. As shown in **Figures 4c** and **4d**, the decreased levels of the typical pro-inflammatory cytokines TNF-α and IL-1β in the FeCCL group compared with the H_2O_2 group showed that the PB family nanozyme possibly played an important role in corneal inflammation suppression.[35] Meanwhile, combining the slightly increased levels of IL-10 (**Figure 4e**) in the FeCCL group compared to the H_2O_2 group, it could be concluded that nanozyme-CCLs could heal damaged corneal tissues by decreasing pro-inflammatory cytokines and increasing anti-inflammatory cytokines, showing that wearing nanozyme-CCL was an effective strategy for OSD prevention and inflammation regulation.[36] Moreover, the biocompatibility of nanozyme-CCLs *in vivo* was evaluated through the blood chemistry analysis of SD rats wearing CCLs without H_2O_2 treatment, which revealed no significant difference in the levels of kidney function

indicators (blood urea nitrogen (BUN) and creatinine (CREA)) and liver function indicators (alanine transaminase (ALT) and aspartate transaminase (AST)), as shown in **Figures 4f-i**.[37]

Therefore, all the multicolor PB family nanozyme-CCLs could protect the cornea from H_2O_2-induced damage through their multienzyme-like activities. Notably, it is believed that more OSDs prevention CCLs with multiple colors could be fabricated by the combination of two or more PB family nanozymes.

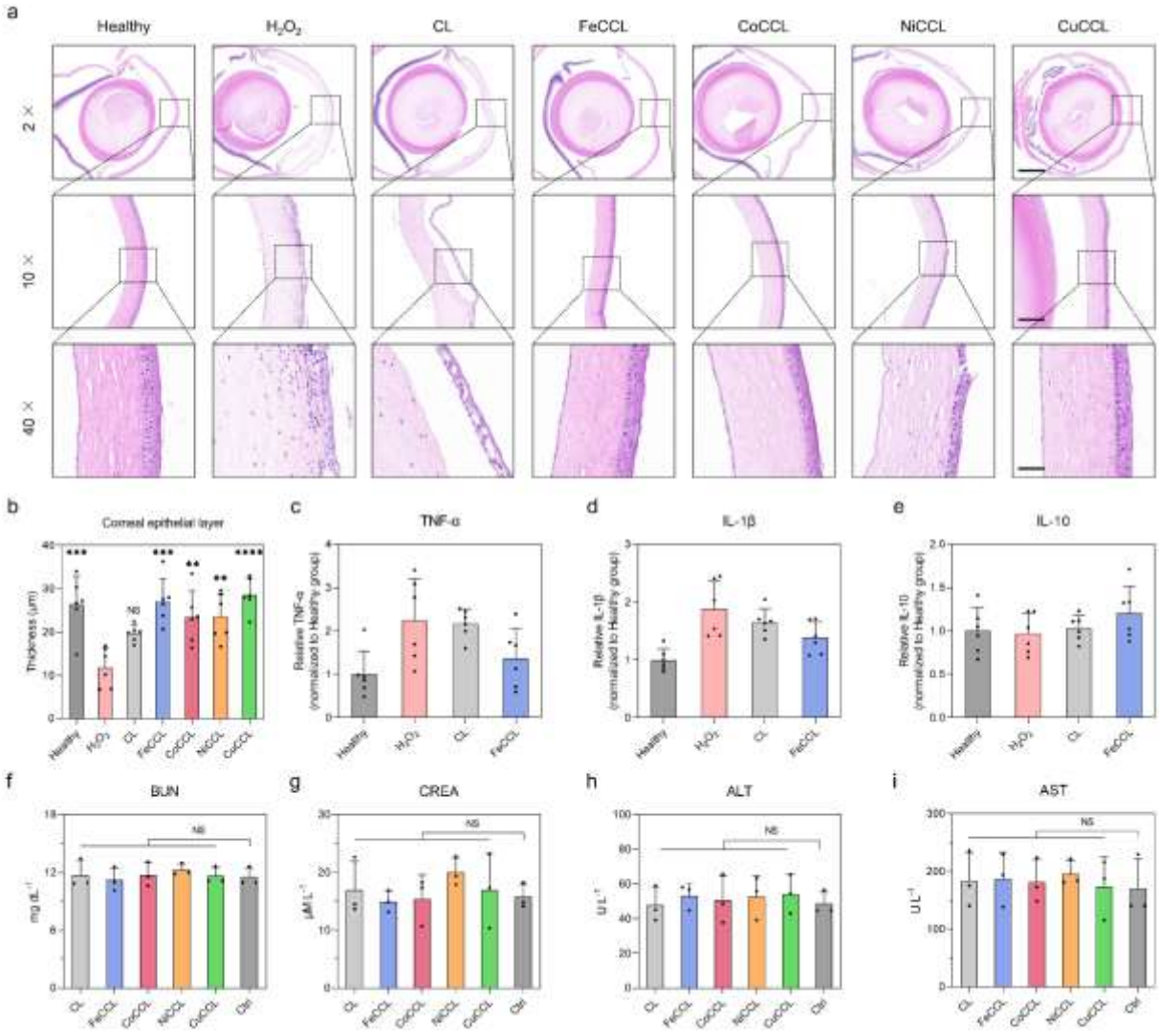

Figure 4. Scavenging ROS to protect the cornea by multicolor PB family nanozyme-CCLs *in vivo*. (a) Representative H&E staining images of corneal tissue from indicated groups (scale bars: 1 mm for 2 ×, 200 μm for 10 ×, and 50 μm for 40 ×). (b) Thickness of corneal epithelial layer in indicated group determined by H&E staining images. Levels of (c) TNF-α, (d) IL-1β, and (e) IL-10 in the indicated groups evaluated by ELISA bioassays. Data are presented as mean ± SD (n = 6). Blood chemistry evaluation of rats wearing CLs. Levels of (f) BUN, (g) CREA, (h) ALT, and (i) AST of indicated groups. Data are presented as mean ± SD (n = 3). The nanozyme-CCLs were prepared using a nanozyme precursor concentration of 0.2 mg mL^{-1}. Statistical differences were analyzed by ordinary one-way analysis of variance (ANOVA): $^{**}P \leq 0.01$, $^{***}P \leq 0.001$, $^{****}P \leq 0.0001$, and NS (not significant). In b, *P* denotes the statistical significance relative to the H_2O_2 group.

To further extend the scope of nanozyme-CCL, we constructed another H_2O_2-induced rabbit model by using blue FeCCL (**Figure 5a**). The model was established using the same protocol as the H_2O_2-induced SD rat model but changed the nanozyme-CCL to larger ones that were suitable for rabbits. Similar to the H&E images shown in **Figure 4a**, a consistent result depicted in H&E images and Masson's trichrome (MT) staining was observed in the rabbit model (**Figures 5b-e**). FeCCL exhibited significant cytoprotective effects, resulting in an improved corneal status (increased corneal epithelial layer thickness and cell density in the epithelial layer, as well as decreased corneal stroma thickness) (**Figures 5f-h**). Moreover, FeCCLs were found to be safe for use on healthy corneas, as confirmed by histological examination of rabbits wearing FeCCLs compared to those wearing CLs or no lenses (**Figure S44**).

Combined with H_2O_2-induced models of both SD rats and rabbits, a set of multicolor PB family nanozyme-CCLs showed great potential in preventing and ameliorating OSDs from potential external insults by effectively scavenging ROS and regulating inflammation. This unique property makes it possible to avoid the intrinsic inflammatory response commonly associated with conventional CCLs and protect individuals at high risk of developing OSDs.

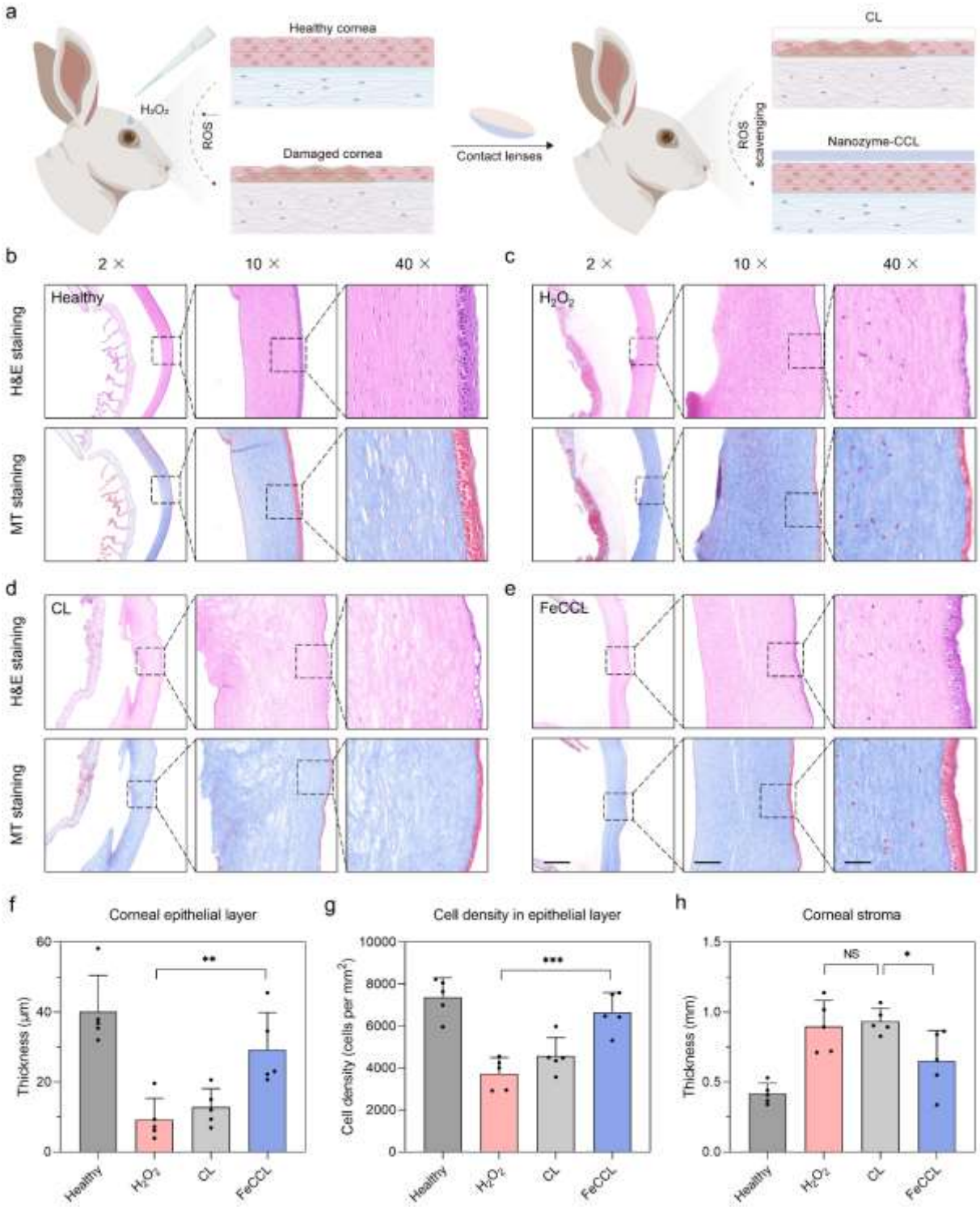

Figure 5. OSDs prevention to protect corneas by blue PB nanozyme-CCL *in vivo*. (a) Schematic of the H_2O_2-induced rabbit model for evaluating the OSDs prevention effect of FeCCL. (b-e) Representative H&E and MT staining images of corneal tissue from indicated groups (scale bars: 1 mm for 2 ×, 200 μm for 10 ×, and 50 μm for 40 ×). (f) Thickness of corneal epithelial layer, (g) cell density in epithelial layer, and (h) thickness of corneal stroma of indicated group determined by H&E and MT staining images. The nanozyme-CCLs were prepared using a nanozyme precursor concentration of 0.2 mg mL^{-1}. Data are presented as mean ± SD (n = 5). Statistical differences were analyzed by ordinary one-way analysis of variance (ANOVA): $*P \leq 0.05$, $**P \leq 0.01$, $***P \leq 0.001$, and NS (not significant).

3. Conclusion

In conclusion, multicolor PB family nanozymes with ROS scavenging abilities were prepared successfully and then embedded into a clinical pHEMA host matrix to fabricate multicolor nanozyme-CCLs. The critical physical properties of nanozyme-CCLs, including diameter, central thickness, base curve, and weight, were fully investigated. Notably, the multienzyme-like activities were well retained in nanozyme-CCLs. The biosafety of nanozyme-CCLs was evaluated from the levels of leaked metal ions, cytocompatibility, and biocompatibility. In addition, SD rat and rabbit models were utilized to demonstrate the bioprotective effects of nanozyme-CCLs against oxidative stress induced by H_2O_2 and UV exposure. Encouragingly, the multicolor PB family nanozyme-CCLs were effective for ROS scavenging and could be applied for the OSDs prevention. This study not only illustrated nanozyme-CCL to protect corneal tissue from external stimulation and reduce the potent risk of CCLs but also rationally utilized the colors of nanozymes.

Experimental Section

Detailed experimental materials and methods can be found in the Supporting Information.

Supporting Information

Supporting Information is available from the Wiley Online Library or from the author.

Acknowledgements

This work was supported by grants from the National Natural Science Foundation of China (No. 21874129, 22174137, 21874067 and 21722503), the International Scientific Cooperation Project of Jilin Scientific and Technological Development Program (No. 20200801044GH), the Key Research and Development Projects of Jilin Scientific and Technological Development Program (No. 202102041266YY), the National Key R&D Program of China (2019YFA0709200 and 2021YFF1200700), Jiangsu Provincial Key R&D Program (BE2022836), and Fundamental Research Funds for the Central Universities (202200325 and 021314380195).

Author contributions

Y. Du and H. Wei conceived the project. Y. Du, H. Wei, and Q. Liu designed the experiments. Q. Liu, S. Zhao, Y. Zhang, Q. Fang, W. Liu, R. Wu, and G. Wei performed the experiments. Q. Liu, S. Zhao, Y. Zhang, and W. Liu analyzed the results. Y. Du, H. Wei, and Q. Liu wrote the manuscript. All authors discussed the results and commented on the manuscript.

Competing interests

Patent application is in progress.

Data availability

Data to support the conclusions in the manuscript can be provided on request.

References

[1] Y. Y. Leong, L. Tong, *Ocul. Surf.* **2015**, *13*, 103.

[2] a) F. Song, S. Hao, Y. Gu, K. Yao, Q. Fu, *Adv. Ophthalmol. Pract. Res.* **2021**, *1*, 100001; b) A. Shoham, M. Hadziahmetovic, J. L. Dunaief, M. B. Mydlarski, H. M. Schipper, *Free Radical. Biol. Med.* **2008**, *45*, 1047; c) E. Generali, L. Cantarini, C. Selmi, *Clin. Rev. Allergy Immunol.* **2015**, *49*, 263; d) M. Markoulli, J. Flanagan, S. S. Tummanapalli, J. Wu, M. Willcox, *Ocul. Surf.* **2018**, *16*, 45; e) I. K. Gipson, *Invest. Ophthalmol. Vis. Sci.* **2013**, *54*, ORSF48.

[3] C. Baudouin, M. Kolko, S. Melik-Parsadaniantz, E. M. Messmer, *Prog. Retinal Eye Res.* **2021**, *83*, 100916.

[4] J. Cejkova, M. Vejrazka, J. Platenik, S. Stipek, *Exp. Gerontol.* **2004**, *39*, 1537.

[5] a) G. D. Novack, *Clin. Pharmacol. Ther.* **2009**, *85*, 539; b) A. Macri, C. Scanarotti, A. M. Bassi, S. Giuffrida, G. Sangalli, C. E. Traverso, M. Iester, *Graefes Arch. Clin. Exp. Ophthalmol.* **2015**, *253*, 425; c) V. V. Brzheskiy, E. L. Efimova, T. N. Vorontsova, V. N. Alekseev, O. G. Gusarevich, K. N. Shaidurova, A. A. Ryabtseva, O. M. Andryukhina, T. G. Kamenskikh, E. S. Sumarokova, E. S. Miljudin, E. A. Egorov, O. I. Lebedev, A. V. Surov, A. R. Korol, I. O. Nasinnyk, P. A. Bezditko, O. P. Muzhychuk, V. A. Vygodin, E. V. Yani, A. Y. Savchenko, E. M. Karger, O. N. Fedorkin, A. N. Mironov, V. Ostapenko, N. A. Popeko, V. P. Skulachev, M. V. Skulachev, *Adv. Ther.* **2015**, *32*, 1263.

[6] Y. Zhu, S. Li, J. Li, N. Falcone, Q. Cui, S. Shah, M. C. Hartel, N. Yu, P. Young, N. R. de Barros, Z. Wu, R. Haghniaz, M. Ermis, C. Wang, H. Kang, J. Lee, S. Karamikamkar, S. Ahadian, V. Jucaud, M. R. Dokmeci, H. J. Kim, A. Khademhosseini, *Adv. Mater.* **2022**, *34*, e2108389.

[7] a) H. Wei, L. Z. Gao, K. L. Fan, J. W. Liu, J. Y. He, X. G. Qu, S. J. Dong, E. K. Wang, X. Y. Yan, *Nano Today* **2021**, *40*, 101269; b) J. Wu, X. Wang, Q. Wang, Z. Lou, S. Li, Y. Zhu, L. Qin, H. Wei, *Chem. Soc. Rev.* **2019**, *48*, 1004.

[8] Y. E. Kim, J. Kim, *ACS Appl. Mater. Interfaces* **2021**, *14*, 23002.

[9] a) D. Chao, Q. Dong, Z. Yu, D. Qi, M. Li, L. Xu, L. Liu, Y. Fang, S. Dong, *J. Am. Chem. Soc.* **2022**, *144*, 23438; b) C. Cheng, Y. Cheng, S. Zhao, Q. Wang, S. Li, X. Chen, X. Yang, H. Wei, *Bioconjug. Chem.* **2022**, *33*, 248; c) Y. Zhao, S. Song, D. Wang, H. Liu, J. Zhang, Z. Li, J. Wang, X. Ren, Y. Zhao, *Nat. Commun.* **2022**, *13*, 6758.

[10] S. W. Choi, B. G. Cha, J. Kim, *ACS Nano* **2020**, *14*, 2483.

[11] a) W. Zhang, S. Hu, J. J. Yin, W. He, W. Lu, M. Ma, N. Gu, Y. Zhang, *J. Am. Chem. Soc.* **2016**, *138*, 5860; b) J. Zhao, X. Cai, W. Gao, L. Zhang, D. Zou, Y. Zheng, Z. Li, H. Chen, *ACS Appl. Mater. Interfaces* **2018**, *10*, 26108; c) X. Ma, J. Hao, J. Wu, Y. Li, X. Cai, Y. Zheng, *Adv. Mater.* **2022**, *34*, e2106723.

[12] a) N. Saliman, P. Morgan, A. MacDonald, C. Maldonado-Codina, *Cornea* **2020**, *39*, 146; b) S. Singh, D. Satani, A. Patel, R. Vhankade, *Cornea* **2012**, *31*, 777; c) T. Watanabe, M. Uematsu, Y. H. Mohamed, H. Eguchi, S. Imai, T. Kitaoka, *Eye Contact Lens* **2018**, *44 Suppl 1*, S322.

[13] J. Chen, Q. Wang, L. Huang, H. Zhang, K. Rong, H. Zhang, S. Dong, *Nano Res.* **2018**, *11*, 4905.

[14] T. Liao, W. Chen, H. Liao, L. Chen, *Sol. Energy Mater. Sol. Cells* **2016**, *145*, 26.

[15] A. Gotoh, H. i. Uchida, M. Ishizaki, T. Satoh, S. Kaga, S. Okamoto, M. Ohta, M. Sakamoto, T. Kawamoto, H. Tanaka, M. Tokumoto, S. Hara, H. Shiozaki, M. Yamada, M. Miyake, M. Kurihara, *Nanotechnology* **2007**, *18*, 345609.

[16] Y. Chen, G. Mehta, V. Vasiliou, *Ocul. Surf.* **2009**, *7*, 176.

[17] a) T. Zhou, X. Yang, Z. Chen, Y. Yang, X. Wang, X. Cao, C. Chen, C. Han, H. Tian, A. Qin, J. Fu, J. Zhao, *Adv. Sci.* **2022**, *9*, e2105466; b) S. S. Tummanapalli, R. Kuppusamy, J. H. Yeo, N. Kumar, E. J. New, M. D. P. Willcox, *Ocul. Surf.* **2021**, *21*, 37.

[18] P. C. Nicolson, J. Vogt, *Biomaterials* **2001**, *22*, 3273.

[19] J. R. Meakin, D. W. L. Hukins, R. M. Aspden, C. T. Imrie, *J. Mater. Sci.-Mater. Med.* **2003**, *14*, 783.

[20] R. Channa, S. N. Zafar, J. K. Canner, R. S. Haring, E. B. Schneider, D. S. Friedman, *JAMA Ophthalmol.* **2016**, *134*, 312.

[21] J. Jee, H. Kim, *Bull. Korean Chem. Soc.* **2015**, *36*, 2682.

[22] S. Zhao, Y. X. Li, Q. Y. Liu, S. R. Li, Y. Cheng, C. Q. Cheng, Z. Y. Sun, Y. Du, C. J. Butch, H. Wei, *Adv. Funct. Mater.* **2020**, *30*, 2004692.

[23] A. Lin, Q. Liu, Y. Zhang, Q. Wang, S. Li, B. Zhu, L. Miao, Y. Du, S. Zhao, H. Wei, *Anal. Chem.* **2022**, *94*, 10636.

[24] J. Kim, J. Park, Y. G. Park, E. Cha, M. Ku, H. S. An, K. P. Lee, M. I. Huh, J. Kim, T. S. Kim, D. W. Kim, H. K. Kim, J. U. Park, *Nat. Biomed. Eng.* **2021**, *5*, 772.

[25] C. Alvarez-Lorenzo, F. Yanez, R. Barreiro-Iglesias, A. Concheiro, *J. Control. Release* **2006**, *113*, 236.

[26] Q. Wang, C. Cheng, S. Zhao, Q. Liu, Y. Zhang, W. Liu, X. Zhao, H. Zhang, J. Pu, S. Zhang, H. Zhang, Y. Du, H. Wei, *Angew. Chem., Int. Ed.* **2022**, *61*, e202201101.

[27] F. Cao, L. Jin, Y. Gao, Y. Ding, H. Wen, Z. Qian, C. Zhang, L. Hong, H. Yang, J. Zhang, Z. Tong, W. Wang, X. Chen, Z. Mao, *Nat. Nanotechnol.* **2023**, *18*, 617.

[28] M. A. Busquets, J. Estelrich, *Drug Discov. Today* **2020**, *25*, 1431.

[29] Y. Matsumura, H. N. Ananthaswamy, *Toxicol. Appl. Pharmacol.* **2004**, *195*, 298.

[30] a) T. L. de Jager, A. E. Cockrell, S. S. Du Plessis, in *Ultraviolet Light in Human Health, Diseases and Environment*, DOI: 10.1007/978-3-319-56017-5_2 (Ed: S. I. Ahmad), Springer International Publishing, Cham **2017**, p. 15; b) C. Zinflou, P. J. Rochette, *Free Radical. Biol. Med.* **2017**, *108*, 118.

[31] C. Liu, T. Miyajima, G. Melangath, T. Miyai, S. Vasanth, N. Deshpande, V. Kumar, S. Ong Tone, R. Gupta, S. Zhu, D. Vojnovic, Y. Chen, E. G. Rogan, B. Mondal, M. Zahid, U. V. Jurkunas, *Proc. Natl. Acad. Sci. U. S. A.* **2020**, *117*, 573.

[32] N. Liu, X. Zhang, N. Li, M. Zhou, T. Zhang, S. Li, X. Cai, P. Ji, Y. Lin, *Small* **2019**, *15*, e1901907.

[33] F. Memarzadeh, N. Shamie, R. N. Gaster, R. S. Chuck, *Ophthalmology* **2004**, *111*, 1546.

[34] J. Li, S. Du, Y. Shi, J. Han, Z. Niu, L. Wei, P. Yang, L. Chen, H. Tian, L. Gao, *Exp. Eye Res.* **2021**, *203*, 108399.

[35] a) H. Bai, F. Kong, K. Feng, X. Zhang, H. Dong, D. Liu, M. Ma, F. Liu, N. Gu, Y. Zhang, *ACS Appl. Mater. Interfaces* **2021**, *13*, 42382; b) K. Zhang, M. Tu, W. Gao, X. Cai, F. Song, Z. Chen, Q. Zhang, J. Wang, C. Jin, J. Shi, X. Yang, Y. Zhu, W. Gu, B. Hu, Y. Zheng, H. Zhang, M. Tian, *Nano Lett.* **2019**, *19*, 2812; c) X. Wang, S. Zhang, M. Dong, Y. Li, Q. Zhou, L. Yang, *J. Cell. Physiol.* **2020**, *235*, 10081; d) M. Reim, A. Kottek, N. Schrage, *Prog. Retinal Eye Res.* **1997**, *16*, 183.

[36] D. Hos, F. Bucher, B. Regenfuss, M. Dreisow, F. Bock, L. Heindl, S. Eming, C. Cursiefen, *Am. J. Pathol.* **2016**, *186*, 159.

[37] T. Liu, B. Xiao, F. Xiang, J. Tan, Z. Chen, X. Zhang, C. Wu, Z. Mao, G. Luo, X. Chen, J. Deng, *Nat. Commun.* **2020**, *11*, 2788.

Multicolor Prussian blue family nanozymes with antioxidant abilities were embedded into cosmetic contact lenses to prevent ocular surface diseases, minimize potential safety risk, and protect corneas from external stimulation and underlying systemic diseases via reactive oxygen species scavenging.

Quanyi Liu[a,b], Sheng Zhao[c], Yihong Zhang[c], Qi Fang[a,b], Wanling Liu[c], Rong Wu[a,b], Gen Wei[c], Hui Wei[c,d]*, and Yan Du[a,b]*

Nanozyme-Cosmetic Contact Lenses for Ocular Surface Diseases Prevention